BIOCHEMISTRY
including biophysical chemistry & molecular biology

Article

pubs.acs.org/biochemistry

Remote Exosites of the Catalytic Domain of Matrix Metalloproteinase-12 Enhance Elastin Degradation

Yan G. Fulcher and Steven R. Van Doren*

Department of Biochemistry, 117 Schweitzer Hall, University of Missouri, Columbia, Missouri 65211, United States

Supporting Information

ABSTRACT: How does matrix metalloproteinase-12 (MMP-12 or metalloelastase) degrade elastin with high specific activity? Nuclear magnetic resonance suggested soluble elastin covers surfaces of MMP-12 far from its active site. Two of these surfaces have been found, by mutagenesis guided by the BINDSIght approach, to affect degradation and affinity for elastin substrates but not a small peptide substrate. Main exosite 1 has been extended to Asp124 that binds calcium. Novel exosite 2 comprises residues from the II−III loop and β-strand I near the back of the catalytic domain. The high degree of exposure of these distal exosites may make them accessible to elastin made more flexible by partial hydrolysis. Importantly, the combination of one lesion each at exosites 1 and 2 and the active site decreased the catalytic competence toward soluble elastin by 13−18-fold to the level of MMP-3, homologue and poor elastase. Double-mutant cycle analysis of conservative mutations of Met156 (exosite 2) and either Asp124 (exosite 1) or Ile180 (active site) showed they had additive effects. Compared to polar substitutions observed in other MMPs, Met156 enhanced affinity and Ile180 the k_{cat} for soluble elastin. Both residues detracted from the higher folding stability with polar mutations. This resembles the trend in enzymes of an inverse relationship between folding stability and activity. Restoring Asp124 from combination mutants enhanced the k_{cat} for soluble elastin. In elastin degradation, exosites 1 and 2 contributed in a manner independent of each other and Ile180 at the active site, but with partial coupling to Ala182 near the active site. The concept of weak, separated interactions coalescing somewhat independently can be extended to this proteolytic digestion of a protein from fibrils.

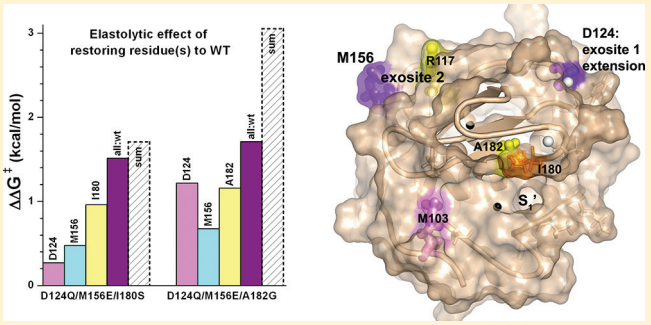

Exosites are pivotal in thrombin recognition of therapeutic inhibitors[1] and peptide substrates from receptors by its catalytic domain.[2] Exosites of MMPs have normally been regarded as residing instead in the noncatalytic C-terminal hemopexin-like domain and fibronectin II-like modules inserted in MMP-2 and -9.[3,4] The additional domains support binding and specificity for substrates from protein fibrils. The hemopexin domain enhances binding and proteolysis of collagen triple helices by several MMPs.[5−11] The fibronectin II-like modules are required for MMP-2 and -9 to bind and digest elastin,[12] gelatin,[8,13] and collagens.[10,14] In contrast, MMP-12 requires only its catalytic domain to degrade elastin. (Mature MMP-12 in vivo retains only its catalytic domain because of the autolytic removal of its hemopexin domain.[15]) What is it about the catalytic domain of MMP-12 that makes it so active upon elastin? Nuclear magnetic resonance (NMR) suggested surfaces of MMP-12 remote from its active site can be covered by soluble α-elastin, such as a strip across the β-sheet and a bowl from helix A to helix C.[16] We investigated whether any of these may function as exosites to support elastin degradation.

Elastin constitutes half the protein mass of the aorta[17] and provides the recoil that dampens the high-pressure waves from heart contraction.[18] Heavy desmosine cross-linking[19] could account for elastin lasting a lifetime. Elastin degradation is characteristic of atherosclerosis,[20] aortic aneurysms, and emphysema (COPD). MMP-12, also known as the metalloelastase secreted by macrophages, has been implicated in each disease.[21−24] Proteolytic release of elastin fragments strongly signals for repair and chronic inflammation by potently attracting leukocytes as in emphysema,[25] stimulating proliferation of lymphocytes, fibroblasts, and smooth muscle cells, and promoting angiogenesis.[24] These are characteristic of age-related arterial aneurysm formation,[24] plus proteolytic clearance of elastin from the aneurysms.[22]

Compared to its closest homologue of the MMP-3 catalytic domain (MMP-3 cd), MMP-12 has a 12−13-fold advantage in elastin degradation in terms of catalytic efficiency, turnover number (k_{cat}), and extent of peptide release.[16,26] Subtleties accounting for this difference have been a topic of investigation. MMP-3 cd has a nearly 3 kcal/mol greater folding stability,[27] in accord with the hypothesis that enzyme variants typically trade stability for activity.[28−30] Millisecond time scale backbone dynamics enveloped the active site of MMP-12 and much more so that of MMP-3 cd.[27]

Received: June 25, 2011
Revised: September 12, 2011
Published: October 3, 2011

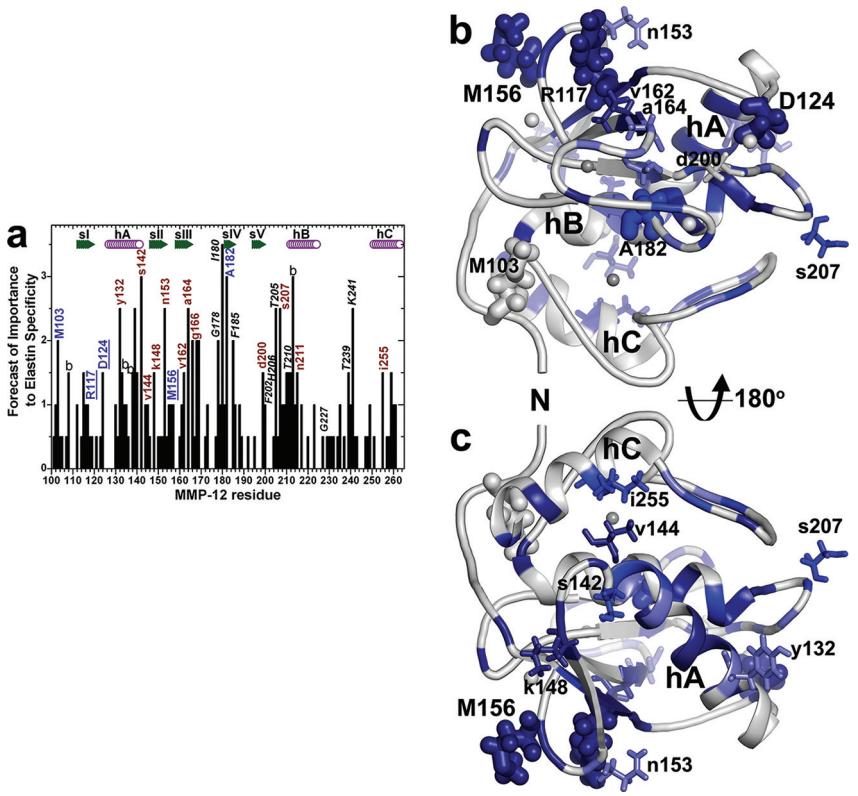

Figure 1. MMP-12 residues distal from the active site chosen for mutagenesis on the basis of putative contacts with 20 kDa α-elastin species (Eln-20) and BINDSIght forecast of importance.[16] (a) Residues were selected for mutagenesis on the basis of this BINDSIght plot suggesting interfaces that could be distinctive. Those with blue and red-brown labels were characterized in this study of remote surfaces and those with black italic labels in the prior study of the active site periphery.[16] The score in the plot accumulated with NMR evidence of surfaces that are covered or perturbed in chemical shift by the Eln-20 binding partner and distinctions in sequence.[16] Uppercase labels mark residues found to support a catalytic efficiency toward fEln-100 higher than that of a conservative mutation, and lowercase labels mark those that do not. Underlined labels mark consequential positions distant from the active site. b denotes a buried residue. (b and c) In the front (b) and back (c) views of the catalytic domain, dark blue, medium blue, and light blue denote strong, medium, and mild protection, respectively, of the surface by Eln-20 from an exogenous Gd·EDTA probe. Side chains are plotted for residues mutated and characterized in this study. Side chains that affected digestion of 100 kDa α-elastin (fEln-100) are drawn with thick sticks and those that did not with thin sticks. Zinc ions are colored darker gray and calcium ions lighter gray.

Among several elastases compared, MMP-12 exhibited the highest affinity for insoluble elastin fibrils.[22] Moreover, most of MMP-12 remained bound even with competition by the TIMP-1 inhibitor of MMPs. MMP-12 was the main MMP observed bound to elastin undergoing digestion in human aortic aneurysms.[22] The notably high affinity for elastin was hypothesized to result from multiple interfaces between MMP-12 and α-elastin that were suggested by NMR.[16]

Within these putative interfaces with α-elastin, the BINDSIght strategy (bioinformatics and NMR discovery of specificity of interactions) predicted at least 28 sequence positions to be potentially distinctive[16] (Figure 1). Ten of these residues from five loops on the perimeter of the active site cleft were investigated and implicated in the enhanced specificity for elastin substrates.[16] The remaining sequence positions distant from the active site are considered here. These candidates are located in the N-terminus through β-strand III, the beginning of the S-shaped III–IV loop, and helix C (Figure 1). Elastin is too amorphous and heterogeneous to crystallize and too repetitious in sequence and too prone to self-association for NMR in solution.[31] Given the barriers to the determination of structures of complexes with elastin, mutagenesis and catalytic characterization have been attractive for evaluating positions in MMP-12 affecting elastin degradation.

Two tools were used in testing if remote residues participate in elastolysis. One tool is the fluor-labeled 100 kDa fraction of α-elastin designated fEln-100. This soluble substrate introduced the ability to compare quantitatively the steady-state kinetics of proteolysis of an elastin substrate.[16,32] fEln-100 retains the heavy desmosine cross-linking of intact elastin fibrils[32−34] and the capacity to self-assemble at physiological temperature.[35] Considering the progression of elastin degradation to clearance[22] via at least three dozen sites of hydrolysis by MMP-12,[36] proteolysis of fEln-100 was suggested to represent later stages of elastolysis when elastin has already been nicked and the fibrils have been partly disrupted.[16]

The second tool is double-mutant cycle analysis of mutational effects on catalysis. It clarifies how additive the effects of mutations may be. Double-mutant cycle analysis applied to enzyme transformation of small molecules showed that well-separated lesions independently impaired the transition-state stabilization; i.e., $\Delta\Delta G_T^{\ddagger}$ is additive.[37] Closely neighboring lesions, on the other hand, have lacked independence and were not energetically additive.[37] When applied to protein−protein interfaces, the additive character of impairments to affinity increased with the distance between lesions.[38] Fully additive behavior was observed for lesions sufficiently separated to reside within independent interfacial clusters[39] or to be free of electrostatic coupling.[38] Mildvan and

dx.doi.org/10.1021/bi2009807 | Biochemistry 2011, 50, 9488–9499

co-workers described different scenarios involving double mutations and insights regarding enzyme mechanism. The energetics of the mutational interactions, defined relative to the wild type as a reference, can be additive, partially additive, synergistic, absent, or antagonistic.[40] Switching to the double mutant as the reference point for comparing mutational effects, called "inverse thinking", simplifies the description of nonadditive effects.[41]

Screening of BINDSIght-proposed sequence positions by mutagenesis has enlarged the remote frontier of the main exosite (now exosite 1) and revealed distant exosite 2 that supports elastolysis by MMP-12. Strategic combination of a mutation in the active site with remote and novel positions in exosites 1 and 2 is enough to diminish selectively the elastolytic activity of MMP-12 by at least its 12-fold margin of superiority versus that of the homologous MMP-3 cd negative control. This approach reached a milestone in engineering elastin specificity out of metalloelastase and strongly suggests specific combinations of well-separated sites of weak interaction with α-elastin that boost the catalytic efficiency of this proteolysis.

EXPERIMENTAL PROCEDURES

Preparation of MMP-12 Variants. The mutations in the human MMP-12 catalytic domain (amino acids 100−263) were generated by QuikChange mutagenesis using PCR master mix (Stratagene). Mutated enzymes were purified as described previously[42] but with an improved folding procedure.[43] Mutant enzymes were stored in small aliquots at −80 °C in 20 mM Tris-HCl (pH 7.5), 10 mM $CaCl_2$, 0.1 mM $ZnCl_2$, 100 mM NaCl, and 50% (w/v) glycerol.

Enzymatic Assays. The concentration of intact enzyme active sites was determined by inhibitor titration of initial velocities[44] with galardin (GM6001, EMD Biosciences) and soluble Knight's peptide substrate FS-6 (EMD).[45] Kinetics of proteolytic digestion of FS-6 and fEln-100[32] were monitored as progress curves at 25 °C with a BioTek Synergy MX plate reader. The fluorescence of FS-6 was excited at 328 nm and monitored at 393 nm. The fluorescence of fEln-100 was excited at 490 nm and detected at 512 nm. All kinetic experiments were performed in TNC buffer [20 mM Tris-HCl (pH 7.5), 10 mM $CaCl_2$, 0.1 mM $ZnCl_2$, 100 mM NaCl, and 0.035% (w/v) Brij-35].

Fitting of Steady-State Enzyme Kinetics. Individual k_{cat}/K_m, K_m, and k_{cat} values were obtained by nonlinear regression and global fitting of two progress curves collected at appropriate concentrations as described in detail previously.[46] The modification of the procedure of fitting the first kinetic phase for fEln-100 has been illustrated.[32]

Release of Peptide from Insoluble Elastin Fibrils. Mutational variants of human MMP-12 were compared by measuring the release of fluorescent peptides from insoluble elastin-fluorescein particles (75−37 μm, Elastin Products Co.); 80 nM enzyme variants were incubated with 2 mg/mL elastin-fluorescein in TNC buffer with gentle shaking at 37 °C for 15 h. The supernatants containing the released fluorescent peptides were diluted 10-fold for fluorescence measurements using the BioTek Synergy MX plate reader with excitation at 490 nm and emission at 520 nm. Measurements of fluorescence from proteolytic release of peptides were first normalized by the fluorescence of substrate-only samples and then expressed as ratios versus wild type MMP-12 controls. Values are given as means ± the standard error of the mean.

Double-mutant cycle analysis. This was performed in the inverse mode to make nonadditive behavior simpler and more intuitive. Inverse thinking uses the double (or triple) mutation as the energetic reference point to highlight the gains from restoring each mutated position to the wild-type sequence.[41] Consequently, changes in transition-state stabilization[47] were calculated from the catalytic efficiencies expressed as

$$\Delta\Delta G_T^{\ddagger} = RT \ln[(k_{cat}/K_m)_{single\_mut} / (k_{cat}/K_m)_{double\_mut}] \quad (1)$$

Likewise, changes in the free energy of substrate binding[40] were approximated as

$$\Delta\Delta G = RT \ln[(1/K_m)_{single\_mut} / (1/K_m)_{double\_mut}] \quad (2)$$

Changes in activation free energy[48] were calculated as

$$\Delta\Delta G^{\ddagger} = RT \ln[(k_{cat})_{single\_mut}/(k_{cat})_{double\_mut}] \quad (3)$$

In inverse thinking, partially additive mutational damage is seen as cooperative because the gain from restoring both mutated residues to those of the wild type exceeds the energetic sum of restoring both residues individually. Synergistic mutational damage is regarded in inverse thinking as anticooperative because the gain in restoring both residues to the native sequence is smaller than the energetic sum of restoring them one at a time. Antagonism is nonadditive behavior that is more obvious in the inverse mode because restoring one residue has the opposite effect of restoring the other residue.[41]

The categories of behavior of combining mutations were identified by the decision tree shown in Figure 4a. For effects to be considered additive (independent), the sum of free energies of restoring each residue individually to that of the wild type needed to agree with the total difference between combined mutation and wild type to within the tolerance ε of 0.2 kcal/mol, as well as within 30%. A sum of single-residue changes back to those of the wild type exceeding restoration of both or all positions back to those of the wild type by more than ε is considered anticooperative[41] (Figure 4a). The sum of restoring single positions to those of the wild type being less than the difference between combined mutation and wild type (by ε at least) is either cooperative of antagonistic. In antagonism, the variant with a combination of mutations outperforms a simpler mutant having a position restored to that of the wild type (Figure 4a).

Affinity for Soluble Elastin. Titrations with α-elastin (Elastin Products Co.) were monitored with intrinsic tryptophan fluorescence emission spectra of MMP-12 variants excited at 280 nm. Elastin is devoid of tryptophan. Each point in titrations was measured with triplicate samples at 25 °C using a BioTek Synergy MX plate reader within 30 min of mixing prior to substantial proteolysis. Fluorescence quenching at 323 nm was normalized by the maximum quenching at the plateau at 2−3 mg/mL α-elastin.

Stability Measurements. The folding stability of selected MMP-12 variants was measured by chemical denaturation using urea at 37 °C and detection of intrinsic tryptophan fluorescence emission; 1.3 μM working stock solutions of each variant of MMP-12 in TNC buffer and TNC buffer with 10 M urea were

mixed and incubated for 10 min to obtain equilibrated solutions with urea concentrations between these extremes. Each mixture was repeated in triplicate. Excitation occurred at 290 nm and emission at 316 nm in the BioTek Synergy MX plate reader. Via the method of Pace,[49] the data were interpreted and the linear transition region was extrapolated to zero denaturant. The folding stability at zero denaturant, $\Delta G(H_2O)$, is

$$\Delta G(H_2O) = \Delta G + m[\text{urea}] \quad (4)$$

where the slope m is the dependence on denaturant concentration.[49]

Normal Mode Analysis. Point mutations were introduced into the coordinates of the lowest-energy NMR structure of human MMP-12(E219A)[50] using PyMol.[51] An anisotropic network model was used to simulate modes of motion using an online server.[52] The modes were compared between the control and mutants by squared fluctuations, deformation energy, and trajectories of motion.

RESULTS

To investigate further why MMP-12 is highly active in digesting proteolysis-resistant elastin substrates, we evaluated the remote regions of its catalytic domain that were covered by soluble α-elastin in an NMR assay.[16]

Selection of Mutations. Recent BINDSIght analysis integrated NMR evidence of MMP-12 surfaces that bind the 20 kDa fraction of α-elastin (Eln-20) with sequence positions distinguishing subfamilies of MMPs.[16] The scores generated from those data suggest the possible importance of sequence positions to elastin interactions (Figure 1a). This study evaluates influences on elastolysis outside the periphery of the active site by surveying broadly the remote sites that have significant BINDSIght scores for putative interactions with Eln-20. The 18 positions not labeled with italics in Figure 1a were mutagenized and their kinetics of digestion of fEln-100 characterized. These include a swath of residues extending from Asn153 and Met156 of the remote II−III loop and Arg117 (top left of Figure 1b) through Val162, Ala164, and Gly166 at β-strand III to calcium-binding Asp124, as well as to Asp200 and Ser207 of the V−B loop (right). Also pictured in Figure 1b are Met103 near the N-terminus and Ala182 at the active site in the center. Flipping the nearly standard view of the enzyme to a back side view (Figure 1c) brings to the foreground mutated residues such as Ile255 of helix C (top), Val144 and Ser142 at the C-terminal end of helix A, Tyr132 at the opposite end of helix A, and Lys148 of β-strand II. These residues were each replaced by the corresponding side chain of a homologous MMP not known to be an elastase. Each of the single-point mutants retained 90−119% of wild-type MMP-12 activity toward soluble Knight's peptide substrate FS-6 (Figure 2a, Table 1, and Table S1 of the Supporting Information) indicating that each remained intact as an MMP.

Mutations Inconsequential to Elastolysis. The point mutants of remote surfaces of MMP-12 protected by Eln-20[16] that retained 84−101% of wild-type activity toward fEln-100 were Y132A, S142E, and V144A at either end of helix A, K148T of β-strand II, N153Y of the II−III loop, and I255V/R of helix C (Figure 1c and Table S1 of the Supporting Information). Consequently, putative contacts of elastin with this region appear unlikely to enhance elastin degradation directly, though they might support the anchoring of MMP-12 to elastin fibrils. Also inconsequential to elastolysis were V162S, A164V, and G166R at and near β-strand III and D200E and

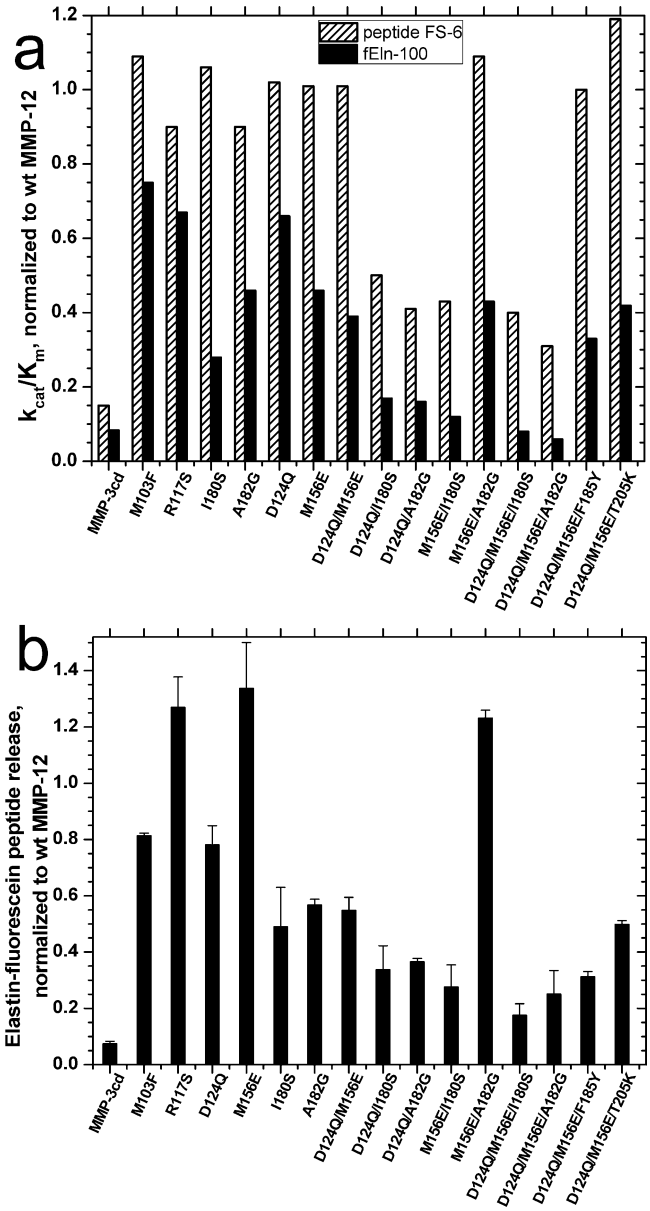

Figure 2. Comparison of activities of single, double, and triple mutants. (a) Catalytic efficiencies of degradation of the soluble α-elastin substrate fEln-100 and the control peptide substrate FS-6. The k_{cat}/K_m values are normalized by the k_{cat}/K_m of wild-type MMP-12 (Table 1). (b) Release of peptides from overnight digestion of fluorescein-tagged, insoluble elastin fibrils normalized by that of wild-type MMP-12.

S207V of the V−B loop on one flank of the active site (Figure 1b and Table S1 of the Supporting Information).

Distal Point Mutations That Selectively Diminish the Extent of Elastolysis. MMP-12 with an M103F mutation at the N-terminus, an R117S mutation in β-strand I, or a D124Q mutation at the C3 calcium binding site[53] in the I−A loop detracted 25, 35, or 35%, respectively, from catalytic efficiency (k_{cat}/K_m) of digestion of fEln-100 (Figure 2a and Table 1). The release of peptide from insoluble elastin fibrils was also modestly weakened by MMP-12(M103F) and MMP-12-(D124Q), but not by MMP(R117S). Adjacent to Arg117 is the M156E lesion of the II−III loop that decreased by 53% the catalytic efficiency toward fEln-100 (Figure 2a and Table 1). It modestly enhanced the release of peptide from insoluble elastin

dx.doi.org/10.1021/bi2009807 | Biochemistry 2011, 50, 9488−9499

Table 1. Catalytic Properties (at 25 °C and pH 7.5) of MMP-12 Variants Found To Have Consequential Mutations

		general substrate FS-6			fEln-100			
MMP-12[a]	location of mutation	k_{cat}/K_m (M^{-1} s^{-1})	k_{cat} (s^{-1})	K_m (μM)	k_{cat}/K_m, (M^{-1} s^{-1})	k_{cat} ($\times 10^{-2}$ s^{-1})	K_m (μM)	relative activity of fEln-100/FS-6 normalized to wt MMP12,[c] selectivity for fEln-100 (%)
wt MMP-12[b]		133800 ± 6000	17.3 ± 0.8	129 ± 4	10690 ± 430	1.06 ± 0.04	1.06 ± 0.04	100.0
wt MMP-3[b]		20660 ± 620	3.2 ± 0.1	154 ± 5	830 ± 40	0.08 ± 0.01	0.94 ± 0.04	50.3
M103F	N-terminus	146300 ± 4400	18.7 ± 0.6	128 ± 4	8040 ± 320	0.92 ± 0.04	1.15 ± 0.04	68.8
R117S	strand I, next to II–III loop	120800 ± 3600	13.7 ± 0.4	113 ± 3	7130 ± 290	0.72 ± 0.03	1.15 ± 0.04	73.8
D124Q	I–A loop, Ca^{2+} ligand	136700 ± 4100	17.1 ± 0.5	125 ± 4	7060 ± 280	1.24 ± 0.05	1.75 ± 0.07	64.6
M156E	II–III loop	135200 ± 4100	16.9 ± 0.5	125 ± 4	4890 ± 200	1.17 ± 0.05	2.39 ± 0.10	45.3
I180S[b]	bulge edge in III–IV loop	141800 ± 4300	24.1 ± 2.2	170 ± 15	2860 ± 140	0.37 ± 0.06	1.3 ± 0.1	25.2
A182G	strand IV	120100 ± 3600	15.6 ± 0.5	130 ± 4	4970 ± 200	0.57 ± 0.02	1.14 ± 0.05	51.8
D124Q/M156E		134700 ± 4000	16.7 ± 0.5	124 ± 4	4210 ± 200	1.43 ± 0.06	3.40 ± 0.14	39.1
D124Q/I180S		67230 ± 2020	16.2 ± 0.5	241 ± 7	1855 ± 80	0.24 ± 0.01	1.27 ± 0.05	34.5
D124Q/A182G		54610 ± 1640	10.6 ± 0.3	194 ± 6	1660 ± 70	0.18 ± 0.01	1.09 ± 0.04	38.1
M156E/I180S		57420 ± 1720	6.8 ± 0.2	119 ± 4	1310 ± 50	0.52 ± 0.02	3.99 ± 0.16	28.6
M156E/A182G		145400 ± 4400	17.2 ± 0.5	118 ± 4	4650 ± 190	2.16 ± 0.09	4.66 ± 0.19	40.0
D124Q/M156E/I180S		53660 ± 1600	9.7 ± 0.3	180 ± 5	829 ± 33	0.10 ± 0.01	1.19 ± 0.05	19.3
D124Q/M156E/A182G		41570 ± 1250	8.4 ± 0.3	202 ± 6	593 ± 24	0.10 ± 0.01	1.71 ± 0.07	17.9
D124Q/M156E/F185Y		133400 ± 4000	18 ± 0.5	135 ± 4	3570 ± 140	0.48 ± 0.02	1.35 ± 0.05	33.5
D124Q/M156E/T205K		159700 ± 4800	18 ± 0.5	113 ± 4	4500 ± 180	0.65 ± 0.03	1.45 ± 0.06	35.3

[a]Each mutation is found at the equivalent position in a less elastolytic homologue such as MMP-3, -8, -10, -11, or -27 or MT-MMP. [b]Previously reported in ref 16. [c]Heights from Figure 2a of black columns divided by hatched columns, i.e., $k_{cat}/K_{m,fEln\text{-}100}/k_{cat}/K_{m,FS\text{-}6}$ after normalization of each k_{cat}/K_m to the wild-type value.

dx.doi.org/10.1021/bi2009807 | Biochemistry 2011, 50, 9488–9499

fibrils (Figure 2b). The new A182G lesion in β-strand IV at the active site served as a positive control that also decreased by 53% the catalytic efficiency toward fEln-100 (Figure 2a and Table 1), a magnitude similar to that of most lesions more peripheral to the active site.[16] The D124Q or M156E lesion eroded activity upon fEln-100 by impairing the K_m and affinity for the substrate (Table 1 and Figure S2 of the Supporting Information). The R117S and A182G lesions instead detracted from catalytic turnover (k_{cat}) (Table 1).

Combinations of Remote and Active Site Mutations. Remote point mutations that selectively decreased activity for the fEln-100 protein substrate were combined with mutations closer to the active site to try to accumulate losses of activity toward fEln-100 without affecting activity for a control peptide substrate. Well-separated mutations that each selectively impair digestion of fEln-100 were chosen for combinations because studies of enzyme catalysis on small molecules[37] and protein−protein affinity[38,39] found mutations to be additive when distant from each other. Two of the three most remote mutations, D124Q (21.6 Å) and M156E (23.6 Å), were combined with mutations at the active site such as I180S (10.0 Å) and A182G (8.4 Å). (In parentheses are listed the distances from their Cα atoms to the active site zinc in the free state in solution.[50]) The M156E substitution is characteristic of MMP-3 (stromelysin 1). The D124Q mutation is native to MMP-8, -10, and -11. The I180S mutation is found in MMP-10 (stromelysin 2). The A182G mutation is found in MMP-26 and -27. Asp124 is 15 Å from Ile180 and 13 Å from Ala182. Met156 is 27 Å from Ile180 and 21 Å from Ala182.

All but one combination of two of these well-separated mutations further reduced activity toward both fEln-100 (Figure 2a) and elastin-fluorescein (Figure 2b) beyond the decreases caused by the single mutations, i.e., D124Q/M156E, D124Q/I180S, D124Q/A182G, M156E/I180S, and M156E/A182G. However, MMP-12(M156E/A182G) was like MMP-12(M156E) in retaining at least wild-type activity toward insoluble elastin-fluorescein fibrils (Figure 2b). MMP-12-(M156E/A182G) is also unique in that its k_{cat} for fEln-100 was twice that of the wild type (Table 1). Nonadditive behaviors of combinations with A182G are described further below. Combination of the M156E lesion with either the remote D124Q or active site A182G lesion retained wild-type activity toward the peptide substrate FS-6, while the three other double mutations did not (Figure 2a). These latter three (D124Q/I180S, D124Q/A182G, and M156E/I180S) still selectively diminished activity toward the fEln-100 substrate more than toward the FS-6 peptide substrate. This selectivity was beyond that of single D124Q, M156E, and A182G mutations, which is evident from the decreased ratios of heights of black bars to hatched bars in Figure 2a, expressed as percentages in the last column of Table 1.

MMP-12 variants with apparent K_m values for fEln-100 increased by more than 2-fold (Table 1) were checked for accompanying decreases in affinity for α-elastin (α-elastin has been recommended for elastase assays[54]). Titrations monitoring intrinsic tryptophan fluorescence emission of MMP-12 show saturable binding of α-elastin (Figure S2a of the Supporting Information). Each of these MMP-12 mutants (M156E, D124Q/M156E, M156E/I180S, and M156E/A182G) displayed decreased affinity relative to that of the wild type. This qualitatively agrees with the fitted 2.3−4.4-fold increases in the apparent K_m for fEln-100 (Figure S2b,c of the Supporting Information). The shapes of the association plots do not conform to the shapes of simple 1:1 binding isotherms (Figure S2d of the Supporting Information). This is consistent with the complexities of a collection of binding events at the three dozen sites of hydrolysis in elastin,[36] the variability in affinity for these sites suggested by fast and slow phases of hydrolysis,[32] and the widely varied masses within α-elastin. The M156E lesion appears to be sufficient to account for the decreased affinity. Addition of D124Q appeared to further decrease the affinity for α-elastin slightly (Figure S2b,c of the Supporting Information).

Exosites 1 and 2. MMP-12(D124Q) and each of the combination mutants that include this mutation had their activities toward fEln-100 and elastin-fluorescein selectively diminished (Figure 2 and Table 1). Asp124 is assigned to principal exosite 1 in elastin degradation by the rationale given in Discussion. Reductions in elastolysis by MMP-12(M156E/I180S) and MMP-12(D124Q/M156E) strengthened the case for contributions arising from Met156 and neighboring Arg117 (Figure 2 and Table 1), which form a distinct patch designated exosite 2 (Figure 3).

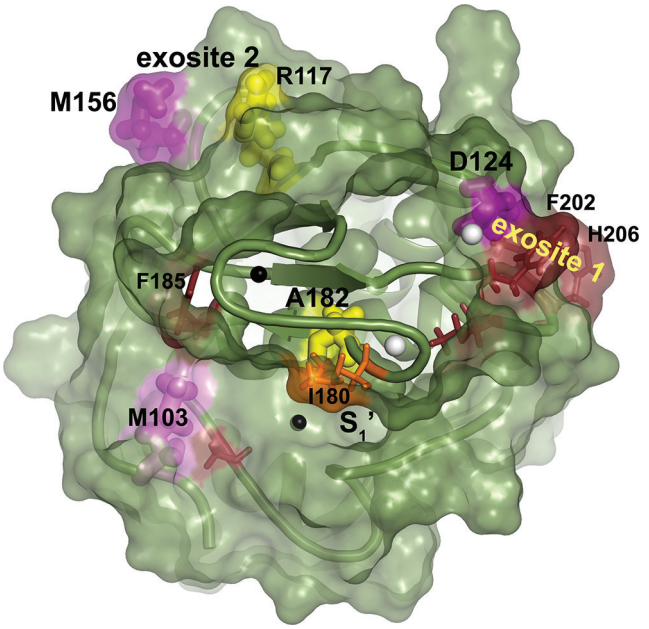

Figure 3. Residues from exosites that enhance elastin degradation. Newly identified residues are colored pink or yellow and labeled with larger type. Adjoining residues identified previously are colored dark red or orange and labeled with smaller type. Residues found to enhance K_m are colored purple and those found to enhance k_{cat} yellow, both with side chains plotted with large bonds. Residues previously found to enhance K_m are colored dark red and those found to enhance k_{cat} orange,[16] both with small bonds. Zinc ions are colored black and calcium ions white. The S-shaped III−IV loop is in the foreground.

Triple Mutations. In an effort to reduce the elastase activity of MMP-12 to the level of its closest homologue of MMP-3 cd, third mutations were added to the lesions in exosites 1 and 2 of MMP-12(D124Q/M156E). Importantly, the triple mutations combining one lesion each at exosites 1 and 2 with one bordering the central region of the active site, namely, D124Q/M156E/I180S and D124Q/M156E/A182G, each conferred a significantly greater loss of catalytic efficiency in digesting fEln-100 than the parental double mutant, D124Q/M156E (Figure 2). The impairment of digestion of elastin

dx.doi.org/10.1021/bi2009807 | Biochemistry 2011, 50, 9488−9499

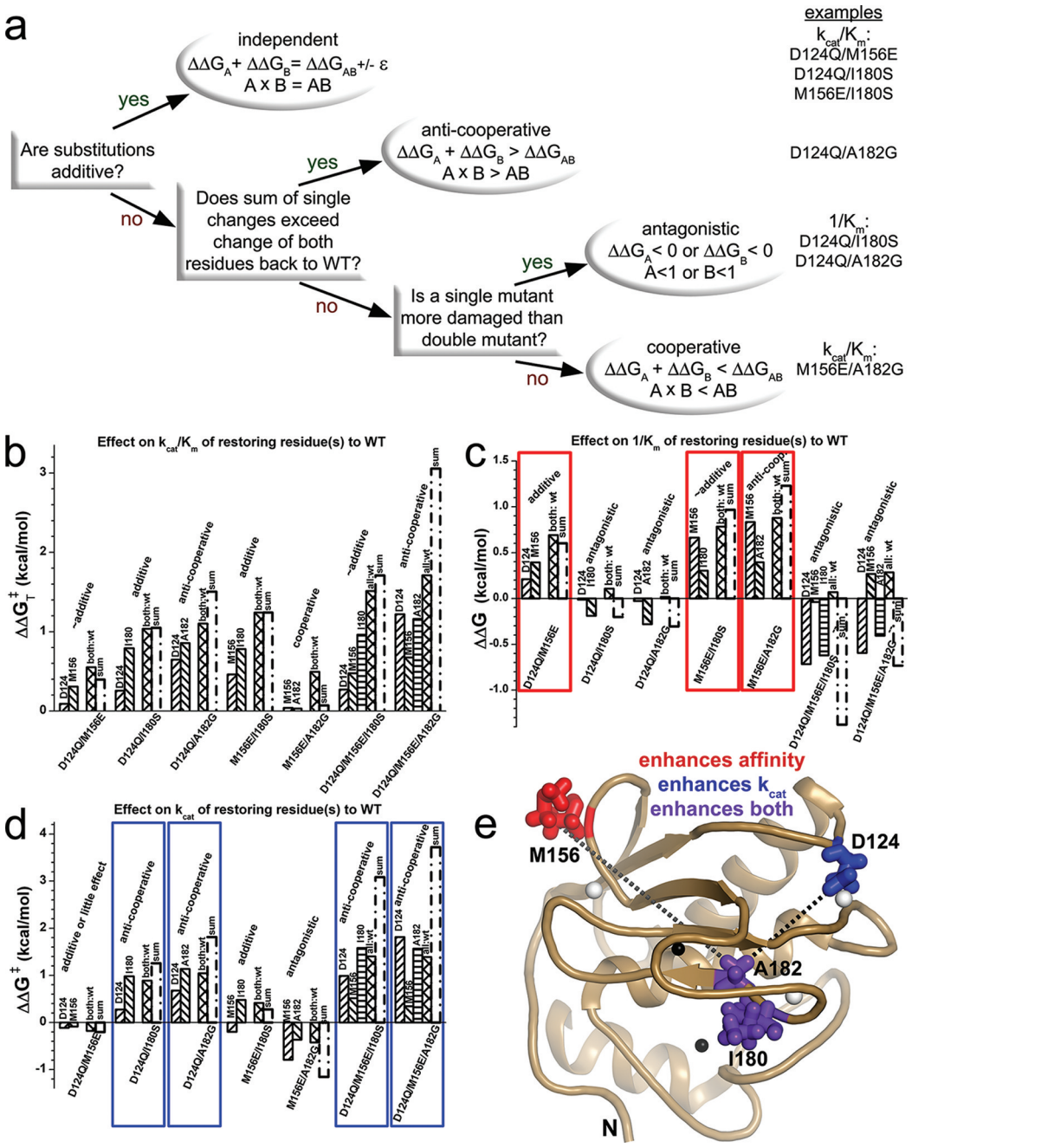

Figure 4. Double-mutant cycle analysis, in the inverse mode,[41] of effects on catalytic turnover of fEln-100 of restoring mutated positions to the wild-type human MMP-12 sequence. (a) Decision tree for categorizing the behaviors. Examples of each behavior are listed at the right. A or B refers to the ratio given as the argument of the ln function of eq 1, 2, or 3 for a single mutant relative to the double mutant reference. AB refers to the ratio of the wild type relative to the double mutant. (b–d) Free energy comparisons are shown for k_{cat}/K_m (b), $1/K_m$ (c), and k_{cat} (d) for fEln-100 and using eq 1, 2, or 3. The restored wild-type residue is labeled above each column. The double or triple mutant reference point is listed below the columns. For example, the first column in panel b reports the difference between M156E and D124Q/M156E variants, which restored D124 to the single mutant. The sum of each free energy from each single residue restored to that of the wild type is marked. The measurement of fully wild type is marked in the comparisons with cross-hatched columns labeled as either both:wt (relative to double mutants) or all:wt (relative to triple mutants). (e) Major trends mapped onto the NMR structure.[50] Red and blue spheres highlight combinations whose contributions to catalytic efficiency are mainly through affinity ($1/K_m$) and catalytic turnover (k_{cat}), respectively. Purple spheres represent side chains that support k_{cat} (d) and also enhance affinity for fEln-100 relative to double mutants with M156E (c). Dotted lines in panel e represent nonadditive coupling with the Ala182 position that is anticooperative with Asp124 (black) or cooperative with Met156 (gray) with respect to catalytic efficiency. Omission of dotted lines among Asp124, Met156, and Ile180 indicates their independent (additive) effects on k_{cat}/K_m.

substrates by these triple mutants was greater than toward the general peptide substrate, which is evident in the decreases in selectivity of at least 2-fold (Table 1). MMP-12(D124Q/M156E/I180S) and MMP-12(D124Q/M156E/A182S) acting on fEln-100 each had k_{cat} values decreased by almost 11-fold and k_{cat}/K_m decreased by 13- and 18-fold, respectively (Table 1). While these two triple mutants displayed less activity toward fEln-100 than the negative control of MMP-3 cd, they retained

dx.doi.org/10.1021/bi2009807 | Biochemistry 2011, 50, 9488–9499

2−2.6-fold more activity toward the FS-6 peptide (Table 1), i.e., competence as an MMP. These results suggested the combined importance of exosites 1 and 2 and the active site in the specific activity of MMP-12 for elastin-derived substrates.

In contrast, adding a third mutation to MMP-12(D124Q/M156E) on the periphery of the active site, whether F185Y near unprimed subsites or T205K beyond primed subsites at the opposite end of the cleft, further decreased only slightly the rate of hydrolysis of either fEln-100 or elastin-fluorescein (Figure 2 and Table 1). MMP-12(D124Q/M156E/F185Y) and MMP-12(D124Q/M156E/T205K) were much less compromised (k_{cat}/K_m decreased by 3- and 2.4-fold, respectively) than those with the third lesion (I180S and A182Q) closer to the catalytic center. The triple mutations with an F185Y or T205K substitution experienced only modest decreases in selectivity for fEln-100 (Table 1) and elastin-fluorescein (Figure 2b).

Double-Mutant Cycle Analysis. This approach tested the hypothesis that elastin interaction and degradation result from a sum of weak interactions. Potentially modular, weak interactions can be tested by simple combinations of two mutations. The inverse mode of double-mutant cycle analysis was employed. It yields the free energies of single mutations and the wild type relative to the reference point of the double mutant. Single mutations are regarded as restoring the wild-type residue[41] (listed above the columns in Figure 4b−d). Combinations of Asp124, Met156, and Ile180 had additive effects on transition-state stabilization ($\Delta\Delta G_T^{\ddagger}$); i.e., they independently promoted the catalytic efficiency (k_{cat}/K_m) of hydrolysis of fEln-100 (Figure 4a,b). Met156 did so by enhancing affinity ($1/K_m$) for fEln-100 compared with that of double mutants (Figure 4c, red boxes). Met156 combined with either Asp124 or Ile180 was essentially independent and additive with respect to $1/K_m$ and k_{cat} (Figure 4c,d). The enhancements of catalytic efficiency by restoring Asp124 relative to double or triple mutants mainly increased the rate of catalytic turnover (blue boxes in Figure 4d and Table 1). Increases in k_{cat}/K_m by Ile180 resulted from enhancements in both affinity and k_{cat} (Figure 4c−e).

In contrast, combinations of mutations involving Ala182 show nonadditive effects on catalytic efficiency ($\Delta\Delta G_T^{\ddagger}$) (Figure 4b). This implies functional coupling of Ala182 with the Asp124 and Met156 positions (signified by dashed lines in Figure 4e). Like Ile180, Ala182 improved k_{cat} and $\Delta\Delta G^{\ddagger}$ (blue boxes in Figure 4d and Table 1) relative to two of three multiple mutations. Two double mutants and two triple mutants each containing the D124Q lesion and either I180S or A182G shared the pattern of antagonism of affinity [$1/K_m$ (Figure 4c)] and anticooperative influences on catalytic turnover (Figure 4d). Among the I180S-containing combination mutants, the effects on affinity and k_{cat} were compensatory, achieving additive effects on transition-state stabilization, i.e., independent effects on catalytic efficiency (Figure 4b). The A182-containing combination mutants fell short of this independence.

F185Y and T205K are effectual point mutations on the perimeter of the active site.[16] Among the triple mutants, D124Q/M156E/F185Y and D124Q/M156E/T205K exhibited comparatively weaker and nearly additive effects on catalytic efficiency and turnover number with fEln-100. Their activation free energies, $\Delta\Delta G^{\ddagger}$, were additive and transition-state stabilization $\Delta\Delta G_T^{\ddagger}$ nearly additive (Figure S1 of the Supporting Information). MMP-12(D124Q/M156E/T205K) was, however, no more impaired in terms of catalytic efficiency with fEln-100 than MMP-12(D124Q/M156E) (Table 1, Figure 2a, and Figure S1 of the Supporting Information). The mild antagonism implies coupling between T205K and another lesion, probably D124Q nearby.

Folding Stabilities. Whether effects on protein folding could indirectly affect catalysis was probed in selected variants of MMP-12 by chemical denaturation using urea. The folding stabilities measured at 37 °C by the linear extrapolation method[49] were 6.4 kcal/mol for the wild type, 7.7 kcal/mol for MMP-12(I180S), 5.7 kcal/mol for MMP-12(D124Q/I180S), 9.0 kcal/mol for MMP-12(M156E/I180S), and 6.8 kcal/mol for MMP-12(M156E/A182G) (Figure 5). These stabilities

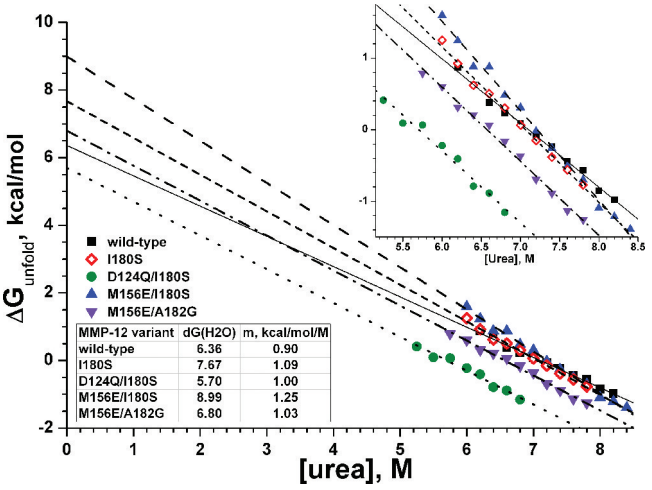

Figure 5. Folding stabilities of selected enzyme variants under chemical denaturation at 37 °C. $\Delta G(H_2O)$ is the free energy needed to unfold the protein in the absence of denaturant that can be accessed by linear extrapolation from the linear unfolding transition region to the *Y*-intercept. The fitted slope of urea concentration dependence is *m* in eq 4.[49] The reproducibility of extrapolated $\Delta G(H_2O)$ observed was $1\sigma \approx 3\%$. The inset shows an expanded view of the transition region.

strongly suggest that MMP-12 remained folded in the presence of D124Q, M156E, I180S, and A182G substitutions. Introduction of the D124Q lesion into MMP-12(I180S) destabilized it by 2 kcal/mol (Figure 5), consistent with removal of the carboxylate side chain from binding the calcium ion at C3 sites. MMP-12(I180S) was 1.3 kcal/mol more stable than the wild type. MMP-12(M156E/I180S) was 2.6 kcal/mol more stable than the wild type, while losing 8-fold of its activity toward fEln-100, 3.6-fold toward elastin-fluorescein fibrils, and 2.3-fold toward the general peptide substrate FS-6. This behavior follows a trend among variants of diverse enzymes in which trade-offs between activity and stability were observed.[28−30]

Robustness of Dynamics. The question of whether mutations might influence indirectly by perturbing dynamics was considered. Normal mode analysis found no differences in simulated modes of motion to result from either the D124Q or I180S substitution. In the fourth lowest mode, a 2% increase in the amplitude of squared fluctuations of distant Thr154 seemed to result from the A182G mutation. Differences in squared fluctuations of Pro104 and Thr154 accompanied the M156E substitution in the sixth, eighth, and tenth lowest modes. Differences from M156E at Phe171 and Asp175 of the S-shaped loop and Ser189 of the IV−V loop were also present in

dx.doi.org/10.1021/bi2009807 | *Biochemistry* 2011, 50, 9488−9499

mode 8 (Figure S3 of the Supporting Information). Apparent changes from this mutation were 2−3-fold larger in mode 8 than in mode 6. The fluctuations of mode 8 with the M156E mutation are portrayed in Movie S1 of the Supporting Information. M156E could have small effects on the dynamics of neighboring loops, but these are not at the active site.

DISCUSSION

Weak, Additive Interactions outside the Active Site in Enzyme Transformation of a Protein. Protein−protein interfaces have been parsed into multiple modules that are each comparatively weak in affinity.[39] Enzymes interacting specifically with small molecule substrates are thought to employ several weak interactions within their active sites. The mutagenesis described here and NMR results[16] strongly suggest that macromolecular substrates derived from elastin extend far beyond the active site in their contacts with MMP-12, thereby influencing both catalytic efficiency and Michaelis constant K_m. The demonstration herein of distant sites (Figure 3) independently supporting the action of an enzyme on a protein substrate comes by way of co-adding contributions of exosites 1 and 2 and the active site periphery in catalytic efficiency upon fEln-100 (Figure 4). This fits conceptually alongside past demonstrations of additive behaviors in enzyme transformation of small molecules and in protein−protein interactions. Common to these diverse scenarios is evidence of separated, weak contacts conferring affinity and adjustable specificity. The modest sizes of effects on catalytic efficiency of a distal exosite 1 or 2 lesion (D124Q or M156E, respectively) are evident as an average transition-state stabilization $\Delta\Delta G_T^{\ddagger}$ of 0.21 ± 0.08 or 0.43 ± 0.08 kcal/mol, respectively, when reversing these respective mutations relative to the multiple mutations [apart from A182G-containing mutants (see below)]. These impairments of elastin degradation are similar in size to those of single-point mutations described on the periphery of the active site.[16] Ile180 and Ala182 closer to the active site contribute more on average to $\Delta\Delta G_T^{\ddagger}$, 0.82 ± 0.09 and 0.63 ± 0.49 kcal/mol, respectively, relative to multiple mutants. Combination of D124, M156, or both with either I180 or A182 results in more significant transition-state stabilizations of 1.04−1.71 kcal/mol (Figure 4a), highlighting the phenomenon of additive $\Delta\Delta G_T^{\ddagger}$ values from separate interfaces (Figure 3).

MMP Exosites. This work's identification of functional exosites within the catalytic domain of an MMP complements past findings of exosites in other domains of MMPs for recognition of fibrillar substrates. The fibronectin II-like modules inserted within the V−B loop of MMP-2 and -9 could be viewed as corresponding to exosite 1 as an extreme elaboration of it.[55] Effects of altered V−B loop sequences on collagen triple-helical peptidase activity[7,56,57] can in retrospect be regarded as evidence of the equivalent of exosite 1 being important in collagenolytic MMPs. Exosite 1 and other locations peripheral to the active site cleft are also clearly important to MMP-12 recognition of collagen IV and V triple helices.[11,16] Mutations or removal of exosites from fibronectin II-like modules of MMP-2 or -9[12−14] or exosites of the catalytic domain of MMP-12 (Figure 3)[16] have analogous effects of damaging interactions with fibrillar protein substrates while retaining the catalytic turnover of small peptide substrates that do not reach the remote exosites. Consequently, selective interference in interactions of one MMP with elastin or triple helices may be achievable by targeting antibodies around the equivalent of exosite 1.

Rationale for Asp124 Belonging to Exosite 1 in Elastolysis. Asp124 lies in close van der Waals contact with Phe202, which was previously identified as part of the main exosite.[16] Both Asp124 and Phe202 are ∼9 Å from the side chains of His206 and Thr205 that cluster in the same exosite patch (Figure 3). Joint binding of the C3 calcium ion by the Asp124 and Glu199 carboxyl groups and the Glu199 and Glu201 carbonyl oxygens[58] creates a bridge from Asp124 to the V−B loop containing most of the residues of exosite 1. Consequently, structural proximity and connectivity are the main arguments for including Asp124 in principal exosite 1. Corroborating evidence comes from nonadditive effects on fEln-100 hydrolysis of addition of the T205K mutation to MMP-12(D124Q/M156E) (Figure S1 of the Supporting Information, Table 1, and Figure 2) that suggest coupling to T205K. This probably resulted from the proximity across exosite 1 of the D124Q lesion, because nearby mutations in interfaces have usually been nonadditive.[37−39] The presumed functional, energetic coupling of D124Q and T205K would support their connectivity within the same structural cluster within the protein−protein interface, the concept developed in ref 39. Thus, assignment of Asp124 to exosite 1 in the context of elastin degradation is based on its structural proximity to exosite 1, calcium bridging to the V−B loop, and apparent functional coupling with Thr205.

Role of Asp124. This aspartate that binds the C3 calcium ion with its carboxyl group is conserved in 18 of 23 MMPs and replaced by glutamine or lysine in five not needing it for activity.[53] Substitution of this aspartate with alanine in MMP-26 decreased its affinity for this calcium ion and proteolytic activity.[59] The decreased activity of D124Q-containing MMP-12 mutants for large substrates from elastin (Figures 2−4 and Table 1) implies a functional contribution of this remote aspartate-containing loop that joins β-strand I with helix A in the $\beta-\alpha-\beta$ motif. The functional role for this loop now appears analogous to that of corresponding loops of $\beta-\alpha-\beta$ motifs that support the active site of triosephosphate isomerase or the nucleotide binding site of the Rossman fold.[60] Despite the small defect of MMP-12(D124Q) in affinity for the soluble elastin substrate (Table 1), restoration of Asp124 instead boosted k_{cat} for fEln-100 compared with those of D124Q-containing combination mutants (blue boxes in Figure 4d). Anticooperative k_{cat} behavior of Asp124 combined with either Ile180 or Ala182 in double and triple mutants (Figure 4d) implies that these residues facilitate the same non-rate-limiting step, according to ref 40. This step probably affects catalytic turnover because of the similarity between $\Delta\Delta G^{\ddagger}$ (for k_{cat}) and $\Delta\Delta G_T^{\ddagger}$ (for k_{cat}/K_m) in double-mutant cycle analysis of most D124Q-containing multiple mutants (Figure 4b,d). Consistent with this, changes in K_m for fEln-100 are minimal for these four multiple mutants (Table 1). Because a wild-type level of catalytic efficiency for the peptide substrate is maintained by four of the eight D124Q mutants (Figure 2a and Table 1), the catalytic consequences of the D124Q mutation can be subtle enough to affect only turnover of the cross-linked and proteolysis-resistant elastin substrates. Modest destabilization of the protein fold and/or perturbation of active site structure by the D124Q mutation might have indirectly compromised enzymatic interaction, perhaps by affecting hydrogen bonding of the Ile180−Ala182 region with the backbone of the substrates.

Independence of Exosite 2. The long distances from Met156 to the active site (24 Å to zinc) and exosite 1 (26 Å to Asp124) indicate that it belongs to neither. The additivity of Met156 with either Asp124 or Ile180 in digestion of fEln-100 (Figure 4) implies the independence of their effects on the same step (see ref 40). Considering the size of the K_m effects (Table 1 and Figure 4), this potentially rate-limiting step might be binding and positioning of fEln-100 to support turnover.

Functional Coupling of Ala182 to Asp124 and Met156. Ala182 exhibited functional coupling to Asp124 and Met156 despite separations of 13 and 21 Å, respectively (Figure 4e). The thermodynamic coupling of Ala182 and Asp124 could facilitate the same non-rate-limiting catalytic step in elastolysis by the argument given above. Ala182 and Met156 were cooperative in transition-state stabilization (Figure 4b), anticooperative in affinity for the soluble elastin (Figure 4c), and antagonistic toward k_{cat} (Figure 4d). The latter two observations suggest that Ala182 and Met156 may facilitate the same step.[40] Ala182 hydrogen bonding of the NH group of the scissile bond of a peptide substrate[61] and the enhancement of α-elastin affinity by Met156 further raises the question of whether these two residues might jointly position segments of α-elastin for cleavage.

There is considerable evidence of allostery acting on the prodomain in the activation of a few MMPs.[4] The functional and energetic coupling of Ala182 with the Asp124 and Met156 positions, symbolized by dashed lines in Figure 4e, suggests the possibility of allosteric transmission across the catalytic domain of an MMP, as well. A182G conferring a slight increase in the level of simulated motion to the Thr154 neighbor of Met156 is consistent with the possibility of some transmission between the active site and exosite 2. Belonging to the same large rigid structural cluster has been proposed as a source of the nonadditivity of residues separated by long distances.[62] This may be plausible in that Ala182 could be rigidly connected by the β-sheet to the locales of Asp124 and Met156.

Exosite 2 in Advanced Elastin Digestion. Hydrolysis of insoluble fluorescein-labeled elastin may represent early stages of digestion of rigid fibrils, while digestion of fEln-100 could represent later stages of digestion that make cross-linked chains more flexible.[16] Thus, retention of a high rate of release of peptides from elastin fibrils by MMP-12(R117S), MMP-12(M156E), and MMP-12(M156E/A182G) (Figure 2b) may suggest contacts with these residues to be unimportant initially in elastin degradation when the fibrils remain too rigid to bend around to reach exosite 2. Because Met156, Arg117, and Asp124 are most exposed, they may be the distal contacts most easily reached by elastin made flexible enough by partial hydrolysis.

Trade-Offs between Stability and Activity. The gains in folding stability of 1.3 kcal/mol with MMP-12(I180S) and 2.6 kcal/mol with MMP-12(M156E/I180S) (Figure 5) vis-à-vis their losses of activity (Figure 2) are consistent with the trend of enzyme variants trading away thermal stability for more activity.[28−30] Such a trade-off was also observed when comparing MMP-3 and -12.[26] Both Met156 and Ile180 place a bulky hydrophobic side chain on the surface of MMP-12, something that is typically destabilizing to a protein structure. Substitutions with glutamate and serine at these two positions (native to MMP-3 and -10, respectively) presumably alleviate the energetically unfavorable ordering of waters around the exposed hydrophobic side chains. Natural selection of Met156 and Ile180 appears to have favored high activity of MMP-12 over its stability. Remote Met156 enhances affinity for soluble elastin, while central Ile180 enhances catalytic turnover (Table 1).

Similarity of MMP-12 Triple Mutants to MMP-3 cd. The 2.6 kcal/mol of stabilization of MMP-12(M156E/I180S) is reminiscent of the 2.8 kcal/mol stabilization of MMP-3 cd relative to MMP-12.[26] More importantly, both MMP-12-(D124Q/M156E/I180S) and MMP-12(D124Q/M156E/A182G) resemble MMP-3 cd in terms of catalytic efficiency, turnover number, and K_m for fEln-100 (Table 1 and Figure 2a). Furthermore, these two triple mutants also resemble MMP-3 cd activity toward the peptide substrate, particularly in terms of K_m but also within a factor of 2−3 for turnover number and catalytic efficiency (Table 1). These combinations of three mutations (among 65 differences in sequence) were enough to force MMP-12 into MMP-3-like behavior.

Analogy with Exosites of Thrombin. Thrombin's exosite 1 is accessed by peptide substrates from protease-activated receptors that bend from the active site around to reach it. Affinity for the peptide was disrupted by mutations at either exosite 1 or the active site.[2] The polypeptide inhibitors hirudin, ornithodorin, and rhodnin each extend from the active site and place their basic and hydrophobic groups across exosite 1.[2] The concept of various polypeptide partners bending from the active site around to exosite 1 seems to generalize to MMP-12. Its catalytic turnover of and affinity for substrates from collagen triple helices and α-elastin are clearly enhanced by exosite 1, which is suggestive of bending of otherwise rigid triple helices to allow them to reach exosite 1 in the Michaelis complex.[16] This could be analogous to peptide substrate positions P_4' and P_5' modulating turnover by a serine protease, a cysteine protease, and MMP-2.[63]

Summary. MMP-12 digestion of substrate-derived elastin now appears to be enhanced by a second and more remote exosite centered around Met156 of the II−III loop and Arg117 of β-strand I. Main exosite 1 at the V−B loop should be expanded to include calcium-binding Asp124 of the I−A loop in the context of elastolysis. The importance of exosite 1 to elastolysis by MMP-12 may have analogies with digestion of proteins from fibrils by collagenolytic MMPs and with peptidase activities of some serine and cysteine proteases. Increased catalytic efficiency for soluble elastin results from affinity enhanced by Met156 and catalytic turnover enhanced by Asp124. Met156 sacrifices folding stability, whereas Asp124 enhances it. Ile180 trades away some stability for a higher k_{cat} for substrates from protein fibrils. Combining one lesion each at Asp124 (exosite 1), Met156 (exosite 2), and either Ile180 or Ala182 at the β-strand IV edge of the active site significantly and selectively decreased the catalytic efficiency of turnover of soluble α-elastin to a value less than or equal to that of the negative control of MMP-3 cd, while preserving more activity on a peptide substrate. The net deterioration of elastolysis by these lesions, except for A182G, is additive and gives specific examples of weak interactions widely distributed from the active site to its periphery and exosites 1 and 2 supporting elastolysis. Thus, the concept of additive combinations of weak, separated interactions has now been demonstrated in a proteolytic enzyme transformation of a protein substrate, broadening the range of examples of additive behavior. The importance of the two novel exosites in elastin degradation is underscored by the achievement of MMP-3-like catalytic behavior via only three distantly separated point mutations of MMP-12.

dx.doi.org/10.1021/bi2009807 | *Biochemistry* 2011, 50, 9488−9499

■ ASSOCIATED CONTENT

Supporting Information

Mutants with activities nearly intact (Table S1), double-mutant cycle analysis of triple mutations with a point mutation on either extreme of the active site cleft (Figure S1), affinities for α-elastin of mutants with apparent K_m values increased by at least 2-fold (Figure S2), amplitudes of motions in normal mode 8 before and after the M156E mutation (Figure S3), and normal mode 8 with M156E present (Movie S1). This material is available free of charge via the Internet at http://pubs.acs.org.

■ AUTHOR INFORMATION

Corresponding Author

*E-mail: vandorens@missouri.edu. Telephone: (573) 882-5113. Fax: (573) 882-5635.

Funding

This work was supported by National Institutes of Health Grants R01GM57289 and GM57289-08S1 and American Heart Association Grant 0855714G.

■ ACKNOWLEDGMENTS

We thank Dr. Mark Palmier for expert advice on fitting of steady-state kinetics to enzyme progress curves and insightful comments on the manuscript.

■ ABBREVIATIONS

BINDSIght, bioinformatics and NMR discovery of specificity of interactions; cd, catalytic domain; Eln-20, 20 kDa α-elastin species; fEln-100, 100 kDa fluorescently labeled α-elastin species; MMP, matrix metalloproteinase; TIMP-1, tissue inhibitor of matrix metalloproteinases-1; TNC, Tris, NaCl, and $CaCl_2$; wt, wild type.

■ REFERENCES

(1) Bode, W. (2006) Structure and interaction modes of thrombin. *Blood Cells, Mol., Dis. 36*, 122−130.

(2) Ayala, Y. M., Cantwell, A. M., Rose, T., Bush, L. A., Arosio, D., and Di Cera, E. (2001) Molecular mapping of thrombin-receptor interactions. *Proteins 45*, 107−116.

(3) Overall, C. M. (2002) Molecular determinants of metalloproteinase substrate specificity: Matrix metalloproteinase substrate binding domains, modules, and exosites. *Mol. Biotechnol. 22*, 51−86.

(4) Sela-Passwell, N., Rosenblum, G., Shoham, T., and Sagi, I. (2010) Structural and functional bases for allosteric control of MMP activities: Can it pave the path for selective inhibition? *Biochim. Biophys. Acta 1803*, 29−38.

(5) Clark, I. M., and Cawston, T. E. (1989) Fragments of human fibroblast collagenase. Purification and characterization. *Biochem. J. 263*, 201−206.

(6) Murphy, G., Allan, J. A., Willenbrock, F., Cockett, M. I., O'Connell, J. P., and Docherty, A. J. (1992) The role of the C-terminal domain in collagenase and stromelysin specificity. *J. Biol. Chem. 267*, 9612−9618.

(7) Chung, L., Shimokawa, K., Dinakarpandian, D., Grams, F., Fields, G. B., and Nagase, H. (2000) Identification of the (183)-RWTNNFREY(191) region as a critical segment of matrix metalloproteinase 1 for the expression of collagenolytic activity. *J. Biol. Chem. 275*, 29610−29617.

(8) Patterson, M. L., Atkinson, S. J., Knauper, V., and Murphy, G. (2001) Specific collagenolysis by gelatinase A, MMP-2, is determined by the hemopexin domain and not the fibronectin-like domain. *FEBS Lett. 503*, 158−162.

(9) Knauper, V., Cowell, S., Smith, B., Lopez-Otin, C., O'Shea, M., Morris, H., Zardi, L., and Murphy, G. (1997) The role of the C-terminal domain of human collagenase-3 (MMP-13) in the activation of procollagenase-3, substrate specificity, and tissue inhibitor of metalloproteinase interaction. *J. Biol. Chem. 272*, 7608−7616.

(10) Tam, E. M., Moore, T. R., Butler, G. S., and Overall, C. M. (2004) Characterization of the distinct collagen binding, helicase and cleavage mechanisms of matrix metalloproteinase 2 and 14 (gelatinase A and MT1-MMP): The differential roles of the MMP hemopexin c domains and the MMP-2 fibronectin type II modules in collagen triple helicase activities. *J. Biol. Chem. 279*, 43336−43344.

(11) Bhaskaran, R., Palmier, M. O., Lauer-Fields, J. L., Fields, G. B., and Van Doren, S. R. (2008) MMP-12 Catalytic Domain Recognizes Triple Helical Peptide Models of Collagen V with Exosites and High Activity. *J. Biol. Chem. 283*, 21779−21788.

(12) Shipley, J. M., Doyle, G. A., Fliszar, C. J., Ye, Q. Z., Johnson, L. L., Shapiro, S. D., Welgus, H. G., and Senior, R. M. (1996) The structural basis for the elastolytic activity of the 92-kDa and 72-kDa gelatinases. Role of the fibronectin type II-like repeats. *J. Biol. Chem. 271*, 4335−4341.

(13) Collier, I. E., Krasnov, P. A., Strongin, A. Y., Birkedal-Hansen, H., and Goldberg, G. I. (1992) Alanine scanning mutagenesis and functional analysis of the fibronectin-like collagen-binding domain from human 92-kDa type IV collagenase. *J. Biol. Chem. 267*, 6776−6781.

(14) O'Farrell, T. J., and Pourmotabbed, T. (1998) The fibronectin-like domain is required for the type V and XI collagenolytic activity of gelatinase B. *Arch. Biochem. Biophys. 354*, 24−30.

(15) Shapiro, S. D., Kobayashi, D. K., and Ley, T. J. (1993) Cloning and characterization of a unique elastolytic metalloproteinase produced by human alveolar macrophages. *J. Biol. Chem. 268*, 23824−23829.

(16) Palmier, M. O., Fulcher, Y. G., Bhaskaran, R., Duong, V. Q., Fields, G. B., and Van Doren, S. R. (2010) NMR and bioinformatics discovery of exosites that tune metalloelastase specificity for solubilized elastin and collagen triple helices. *J. Biol. Chem. 285*, 30918−30930.

(17) Starcher, B. C., and Galione, M. J. (1976) Purification and comparison of elastins from different animal species. *Anal. Biochem. 74*, 441−447.

(18) Wagenseil, J. E., and Mecham, R. P. (2009) Vascular extracellular matrix and arterial mechanics. *Physiol. Rev. 89*, 957−989.

(19) Wagenseil, J. E., and Mecham, R. P. (2007) New insights into elastic fiber assembly. *Birth Defects Res., Part C 81*, 229−240.

(20) Robert, L., Robert, A. M., and Jacotot, B. (1998) Elastin-elastase-atherosclerosis revisited. *Atherosclerosis 140*, 281−295.

(21) Hautamaki, R. D., Kobayashi, D. K., Senior, R. M., and Shapiro, S. D. (1997) Requirement for macrophage elastase for cigarette smoke-induced emphysema in mice. *Science 277*, 2002−2004.

(22) Curci, J. A., Liao, S., Huffman, M. D., Shapiro, S. D., and Thompson, R. W. (1998) Expression and localization of macrophage elastase (matrix metalloproteinase-12) in abdominal aortic aneurysms. *J. Clin. Invest. 102*, 1900−1910.

(23) Johnson, J. L., George, S. J., Newby, A. C., and Jackson, C. L. (2005) Divergent effects of matrix metalloproteinases 3, 7, 9, and 12 on atherosclerotic plaque stability in mouse brachiocephalic arteries. *Proc. Natl. Acad. Sci. U.S.A. 102*, 15575−15580.

(24) Antonicelli, F., Bellon, G., Debelle, L., and Hornebeck, W. (2007) Elastin-elastases and inflamm-aging. *Curr. Top. Dev. Biol. 79*, 99−155.

(25) Hunninghake, G. W., Davidson, J. M., Rennard, S., Szapiel, S., Gadek, J. E., and Crystal, R. G. (1981) Elastin fragments attract macrophage precursors to diseased sites in pulmonary emphysema. *Science 212*, 925−927.

(26) Liang, X., Arunima, A., Zhao, Y., Bhaskaran, R., Shende, A., Byrne, T. S., Fleeks, J., Palmier, M. O., and Van Doren, S. R. (2010) Apparent tradeoff of higher activity in MMP-12 for enhanced stability and flexibility in MMP-3. *Biophys. J. 99*, 273−283.

(27) Liang, J., Liu, E., Yu, Y., Kitajima, S., Koike, T., Jin, Y., Morimoto, M., Hatakeyama, K., Asada, Y., Watanabe, T., Sasaguri, Y., Watanabe, S., and Fan, J. (2006) Macrophage metalloelastase accelerates the progression of atherosclerosis in transgenic rabbits. *Circulation 113*, 1993−2001.

(28) Shoichet, B. K., Baase, W. A., Kuroki, R., and Matthews, B. W. (1995) A relationship between protein stability and protein function. *Proc. Natl. Acad. Sci. U.S.A. 92*, 452−456.
(29) Arnold, F. H., Wintrode, P. L., Miyazaki, K., and Gershenson, A. (2001) How enzymes adapt: Lessons from directed evolution. *Trends Biochem. Sci. 26*, 100−106.
(30) Beadle, B. M., and Shoichet, B. K. (2002) Structural bases of stability-function tradeoffs in enzymes. *J. Mol. Biol. 321*, 285−296.
(31) Tamburro, A. M., Bochicchio, B., and Pepe, A. (2005) The dissection of human tropoelastin: From the molecular structure to the self-assembly to the elasticity mechanism. *Pathol. Biol. 53*, 383−389.
(32) Palmier, M. O., Fulcher, Y. G., and Van Doren, S. R. (2011) Solubilized elastin substrate for continuous fluorimetric assay of kinetics of elastases. *Anal. Biochem. 408*, 172−174.
(33) Partridge, S. M., and Davis, H. F. (1955) The chemistry of connective tissues. 3. Composition of the soluble proteins derived from elastin. *Biochem. J. 61*, 21−30.
(34) Mecham, R. P., and Lange, G. (1980) Measurement by radioimmunoassay of soluble elastins from different animal species. *Connect. Tissue Res. 7*, 247−252.
(35) Cox, B. A., Starcher, B. C., and Urry, D. W. (1973) Coacervation of α-elastin results in fiber formation. *Biochim. Biophys. Acta 317*, 209−213.
(36) Taddese, S., Weiss, A. S., Neubert, R. H., and Schmelzer, C. E. (2008) Mapping of macrophage elastase cleavage sites in insoluble human skin elastin. *Matrix Biol. 27*, 420−428.
(37) Wells, J. A. (1990) Additivity of mutational effects in proteins. *Biochemistry 29*, 8509−8517.
(38) Schreiber, G., and Fersht, A. R. (1995) Energetics of protein-protein interactions: Analysis of the Barnase-Barstar interface by single mutations and double mutant cycles. *J. Mol. Biol. 248*, 478−486.
(39) Reichmann, D., Rahat, O., Albeck, S., Meged, R., Dym, O., and Schreiber, G. (2005) The modular architecture of protein-protein binding interfaces. *Proc. Natl. Acad. Sci. U.S.A. 102*, 57−62.
(40) Mildvan, A. S., Weber, D. J., and Kuliopulos, A. (1992) Quantitative interpretations of double mutations of enzymes. *Arch. Biochem. Biophys. 294*, 327−340.
(41) Mildvan, A. S. (2004) Inverse thinking about double mutants of enzymes. *Biochemistry 43*, 14517−14520.
(42) Parkar, A. A., Stow, M. D., Smith, K., Panicker, A. K., Guilloteau, J. P., Jupp, R., and Crowe, S. J. (2000) Large-scale expression, refolding, and purification of the catalytic domain of human macrophage metalloelastase (MMP-12) in *Escherichia coli*. *Protein Expression Purif. 20*, 152−161.
(43) Zheng, X., Ou, L., Tong, X., Zhu, J., and Wu, H. (2007) Over-expression and refolding of isotopically labeled recombinant catalytic domain of human macrophage elastase (MMP-12) for NMR studies. *Protein Expression Purif. 56*, 160−166.
(44) Knight, C. G. (1995) Active-site titration of peptidases. *Methods Enzymol. 248*, 85−101.
(45) Neumann, U., Kubota, H., Frei, K., Ganu, V., and Leppert, D. (2004) Characterization of Mca-Lys-Pro-Leu-Gly-Leu-Dpa-Ala-Arg-NH_2, a fluorogenic substrate with increased specificity constants for collagenases and tumor necrosis factor converting enzyme. *Anal. Biochem. 328*, 166−173.
(46) Palmier, M. O., and Van Doren, S. R. (2007) Rapid determination of enzyme kinetics from fluorescence: Overcoming the inner filter effect. *Anal. Biochem. 371*, 43−51.
(47) Wilkinson, A. J., Fersht, A. R., Blow, D. M., and Winter, G. (1983) Site-directed mutagenesis as a probe of enzyme structure and catalysis: Tyrosyl-tRNA synthetase cysteine-35 to glycine-35 mutation. *Biochemistry 22*, 3581−3586.
(48) Klimacek, M., and Nidetzky, B. (2009) The oxyanion hole of *Pseudomonas fluorescens* mannitol 2-dehydrogenase: A novel structural motif for electrostatic stabilization in alcohol dehydrogenase active sites. *Biochem. J. 425*, 455−463.
(49) Pace, C. N., and Shaw, K. L. (2000) Linear Extrapolation Method of Analyzing Solvent Denaturation Curves. *Proteins: Struct., Funct., Genet. 4* (Suppl.), 1−7.
(50) Bhaskaran, R., Palmier, M. O., Bagegni, N. A., Liang, X., and Van Doren, S. R. (2007) Solution structure of inhibitor-free human metalloelastase (MMP-12) indicates an internal conformational adjustment. *J. Mol. Biol. 374*, 1333−1344.
(51) DeLano, W. L. (2002) *The PyMOL Molecular Graphics System*, DeLano Scientific, Palo Alto, CA.
(52) Eyal, E., Yang, L.-W., and Bahar, I. (2006) Anisotropic network model: Systematic evaluation and a new web interface. *Bioinformatics 22*, 2619−2627.
(53) Maskos, K. (2005) Crystal structures of MMPs in complex with physiological and pharmacological inhibitors. *Biochimie 87*, 249−263.
(54) Keller, S., and Mandl, I. (1971) Solubilized Elastin as a Substrate for Elastase and Elastase Inhibitor Determinations. *Biochem. Med. 5*, 342−347.
(55) Van Doren, S. R. (2011) Structural Basis of Extracellular Matrix Interactions with Matrix Metalloproteinases. In *Extracellular Matrix Degradation* (Parks, W. C., and Mecham, R. P., Eds.) pp 123−144, Springer-Verlag, Berlin.
(56) Pelman, G. R., Morrison, C. J., and Overall, C. M. (2005) Pivotal molecular determinants of peptidic and collagen triple helicase activities reside in the S3′ subsite of matrix metalloproteinase 8 (MMP-8): The role of hydrogen bonding potential of ASN188 and TYR189 and the connecting cis bond. *J. Biol. Chem. 280*, 2370−2377.
(57) Minond, D., Lauer-Fields, J. L., Cudic, M., Overall, C. M., Pei, D., Brew, K., Visse, R., Nagase, H., and Fields, G. B. (2006) The roles of substrate thermal stability and P2 and P1′ subsite identity on matrix metalloproteinase triple-helical peptidase activity and collagen specificity. *J. Biol. Chem. 281*, 38302−38313.
(58) Lang, R., Kocourek, A., Braun, M., Tschesche, H., Huber, R., Bode, W., and Maskos, K. (2001) Substrate specificity determinants of human macrophage elastase (MMP-12) based on the 1.1 Å crystal structure. *J. Mol. Biol. 312*, 731−742.
(59) Lee, S., Park, H. I., and Sang, Q. X. (2007) Calcium regulates tertiary structure and enzymatic activity of human endometase/matrilysin-2 and its role in promoting human breast cancer cell invasion. *Biochem. J. 403*, 31−42.
(60) Branden, C., and Tooze, J. (1999) *Introduction to Protein Structure*, 2nd ed., Garland Publishing, New York.
(61) Bertini, I., Calderone, V., Fragai, M., Luchinat, C., Maletta, M., and Yeo, K. J. (2006) Snapshots of the reaction mechanism of matrix metalloproteinases. *Angew. Chem., Int. Ed. 45*, 7952−7955.
(62) Istomin, A. Y., Gromiha, M. M., Vorov, O. K., Jacobs, D. J., and Livesay, D. R. (2008) New insight into long-range nonadditivity within protein double-mutant cycles. *Proteins: Struct., Funct., Bioinf. 70*, 915−924.
(63) Schilling, O., and Overall, C. M. (2008) Proteome-derived, database-searchable peptide libraries for identifying protease cleavage sites. *Nat. Biotechnol. 26*, 685−694.